Evidence for narrow resonant structures at $W \approx 1.68$ GeV and $W \approx 1.72$ GeV in real Compton scattering off the proton

V. Kuznetsov,[1,*] F. Mammoliti,[2,3] V. Bellini,[2,3] G. Gervino,[4,5] F. Ghio,[6,7] G. Giardina,[8] W. Kim,[9] G. Mandaglio,[2,8] M. L. Sperduto,[2,3] and C. M. Sutera[2,3]

[1]*Petersburg Nuclear Physics Institute, 188300, Gatchina, Russia*
[2]*INFN - Sezione di Catania, via Santa Sofia 64, I-95123 Catania, Italy*
[3]*Dipartimento di Fisica ed Astronomia, Università di Catania, I-95123 Catania, Italy*
[4]*Dipartamento di Fisica Sperimentale, Università di Torino, via P.Giuria, I-00125 Torino, Italy*
[5]*INFN - Sezione di Torino, I-10125 Torino, Italy*
[6]*INFN - Sezione di Roma, piazzale Aldo Moro 2, I-00185 Roma, Italy*
[7]*Instituto Superiore di Sanità, viale Regina Elena 299, I-00161 Roma, Italy*
[8]*Dipartimento di Fisica e di Scienze della Terra - Università di Messina, salita Sperone 31, 98166 Messina, Italy*
[9]*Kyungpook National University, 702-701, Daegu, Republic of Korea*

First measurement of the beam asymmetry Σ for Compton scattering off the proton in the energy range $E_\gamma = 0.85$–1.25 GeV is presented. The data reveal two narrow structures at $E_\gamma = 1.036$ and $E_\gamma = 1.119$ GeV. They may signal narrow resonances with masses near 1.68 and 1.72 GeV, or they may be generated by the subthreshold $K\Lambda$ and ωp production. Their decisive identification requires additional theoretical and experimental efforts.

The observation of a narrow enhancement at $W \sim 1.68$ GeV in η photoproduction [1–5] and Compton scattering off the neutron [6] (the so-called neutron anomaly) is of particular interest because it may signal a nucleon resonance with unusual properties: a mass near $M \sim 1.68$ GeV, a narrow ($\Gamma \leqslant 25$ MeV) width, a strong photoexcitation on the neutron, and a suppressed decay to the πN final state [7–11]. Such resonance was never predicted by the traditional constituent quark model [12]. On the contrary, its properties coincide surprisingly well with those expected for an exotic state predicted in the framework of the chiral soliton model [13–17].

On the other hand, several groups [18] explained the bump in the $\gamma n \to \eta n$ cross section in terms of the interference of well-known wide resonances. Although this assumption was challenged by the results on Compton scattering off the neutron [6] (this reaction is governed by different resonances), it is widely discussed in literature. Another explanation was proposed by Doring and Nakayama [19]. They explained the neutron anomaly as virtual sub-threshold $K\Lambda$ and $K\Sigma$ photoproduction ("cusp effect"). At present, the decisive identification of the narrow peculiarity at $W \sim 1.68$ GeV is a challenge for both theory and experiment.

One benchmark signature of the $N^*(1685)$ resonance (if it does exist) is strong photoexcitation on the neutron and weak (but not zero) photoexcitation on the proton. Such resonance would appear in cross section on the proton as a minor peak (dip) structure which might be not (or poorly) seen in experiment. However, its signal may be amplified in polarization observables due to the interference with other resonances.

The recent high-precision and high-resolution measurement of the $\gamma p \to \eta p$ cross section by the A2@MaMiC Collaboration [20] made it possible to retrieve a small dip at $W \approx 1.69$ GeV which was not resolved in previous experiments. At the same time the revision of the GRAAL beam asymmetry Σ for $\gamma p \to \eta p$ revealed a resonant structure at $W = 1.685$ GeV [21,22] (see also [23,24]). The bump in the Compton scattering off the neutron at $W = 1.685$ GeV was observed at GRAAL [6]. The motivation for this work was to search, in analogy with η photoproduction, a resonant structure in polarization observables for Compton scattering on the proton.

In this Rapid Commnication, we report on the first measurement of the beam asymmetry Σ for Compton scattering off the proton in the range of incident-photon energies $E_\gamma = 0.85$–1.25 GeV. The data were collected at the GRAAL facility [25] from 1998 to 2003 in a number of data-taking periods. The main difference between the periods was the usage of either UV or green laser light. A highly polarized and tagged photon beam was produced by means of backscattering of this light on 6.04 GeV electrons circulating in the storage ring of the European Synchrotron Radiation Facility (ESRF, Grenoble, France). The tagged photon-energy range was $\sim$0.8–1.5 GeV with the UV laser and $\sim$0.65–1.1 GeV with the green one. The linear beam polarization varied from $\sim$40% at the lower energy limits up to $\sim$98% at the upper ones. The results obtained with two different types of runs were then used for cross-checks.

Scattered photons were detected in a cylindrically symmetrical bismuth germanate (BGO) ball [26]. The ball provided the detection of photons emitted at $\theta_{lab} = 25°$–$155°$ with respect to a beam axis. Recoil protons emitted at $\theta_{lab} \leqslant 25°$ were detected in an assembly of forward detectors. It consisted of two planar multiwire chambers, a double hodoscope

---

*Slava@pnpi.spb.ru

scintillator wall, and a lead-scintillator time-of-flight (TOF) wall [27].

The data analysis was similar to that used in the previous measurement on the neutron [6]. At first, the γp final states were identified using the criterion of coplanarity, cuts on the proton and photon missing masses, and comparing the measured TOF and the polar angle of the recoil proton with the same quantities calculated assuming the $\gamma p \to \gamma p$ reaction.

The sample of the selected events was still populated by events from the π^0 photoproduction. Two types of the π^0 background were taken into consideration:

(i) Symmetric $\pi^0 \to 2\gamma$ decays. The pion decays in two photons of nearly equal energies. Being emitted in a narrow cone along the pion trajectory, such photons imitate a single-photon hit in the BGO ball.

(ii) Asymmetric $\pi^0 \to 2\gamma$ decays. One of the photons takes the main part of the pion energy. It is emitted nearly along the pion trajectory. Such photon and the recoil proton mimic Compton scattering. The second photon is soft and is emitted into a backward hemisphere relative to the pion track. Its energy depends on the pion energy and may be as low as 6–10 MeV.

The symmetric events were efficiently rejected by analyzing the distribution of energies deposited in crystals attributed to the corresponding cluster in the BGO ball. The efficiency of this rejection was verified in simulations and found to be 99%. The asymmetric $\pi^0 \to 2\gamma$ decays were the major problem. The GRAAL detector provides the low-threshold (5 MeV) detection of photons in the nearly 4π solid angle. If one (high-energy) photon would be emitted at backward angles, the second (low-energy) photon could then be detected in the BGO ball or in the forward lead-scintillator wall. This feature made it possible to suppress the π^0 photoproduction.

For the further selection of events the missing energy $E_{\rm mis}$ was employed

$$E_{\rm mis} = E_\gamma - E_{\gamma'} - T_p(\theta_p), \qquad (1)$$

where E_γ denotes the energy of the incoming photon, $E_{\gamma'}$ is the energy of the scattered photon, and $T_p(\theta_p)$ is the kinetic energy of the recoil proton.

The simulated spectra of the missing energy are shown in the upper panels of Fig. 1. π^0 events form wide distributions. Compton events generate narrow peaks centered around $E_{\rm mis} = 0$. The events in this region belong to both Compton scattering and π^0 photoproduction. The contamination of events from other reactions (mostly double neutral pion photoproduction) does not exceed 2%. At larger $E_{\rm mis}$ the spectra are dominated by π^0 events.

The Compton peak is clearly seen at 157° (the angular bin 151°–165°). At these angles soft photons from asymmetric π^0 decays are efficiently detected in either the BGO ball or in the forward shower wall. At more forward angles part of such photons escape out through the backward gap in the GRAAL detector. The distributions of Compton and π^0 events get closer being almost unresolved at 131° (the angular bin 122°–137°).

The experimental spectra (lower panels of Fig. 1) are quite similar to the simulated ones. Solid lines show the cut $-0.04 \leqslant E_{\rm mis} \leqslant 0.025$. This cut was used to select the
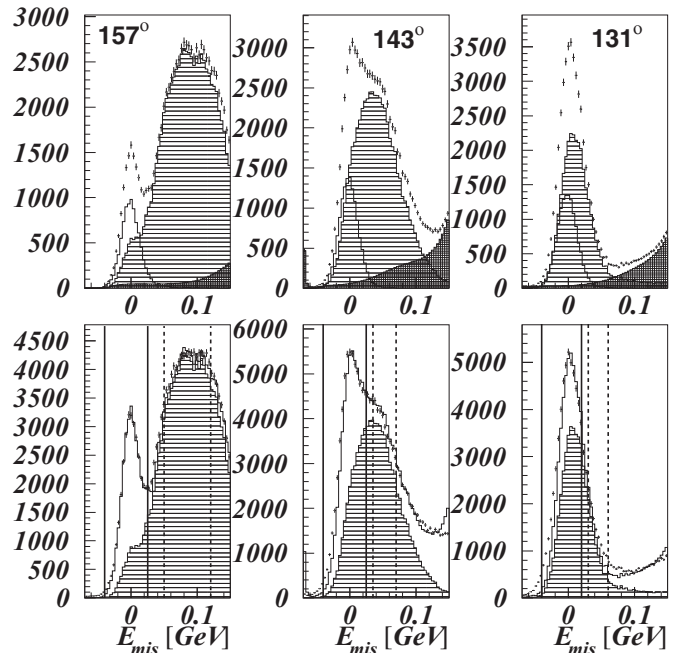

FIG. 1. Spectra of missing energy. Upper panels show the results of simulations. Solid lines correspond to Compton events. Dashed areas are the events from $\gamma p \to \pi^0 p$. Dark areas are the yields of other reactions. Lower panels show the spectra obtained in experiment. Dashed areas are the estimated contamination of π^0 events. Solid lines indicate the cut used to select the mixture of Compton and π^0 events. Dashed lines are the side-band cuts used to select π^0 events.

mixture of Compton and π^0 events. The events in the region above $E_{\rm mis} = 0.035$ GeV are mostly from π^0 photoproduction. Dashed lines in Fig. 1 indicate side-band cuts. These cuts select mostly π^0 events.

Figure 2 shows the beam asymmetry Σ of events selected using the main and side-band cuts. The results obtained with the UV and green lasers are statistically independent. They are in good agreement. The data points obtained with the side-band cuts (right panels of Fig. 2) are close to the SM11 solution of the SAID partial-wave analysis (PWA) for π^0 photoproduction. The minor discrepancy is due to the contamination of Compton and other events. The beam asymmetries of the mixture of Compton and π^0 events (the main cut, left panels of Fig. 2) deviate from the SM11 solution. There are two narrow structures which are not seen with the side-band cuts.

The validity of this observation was verified by means of different cuts of the missing energy in the overall angular range 122°–165°, namely $-0.04 \leqslant E_{\rm mis} < 0$ GeV, $0 \leqslant E_{\rm mis} < 0.025$ GeV, and $0.025 \leqslant E_{\rm mis} < 0.05$ GeV. The first two cuts selected the mixture of Compton and π^0 events. Both structures were seen with these cuts and disappeared with the third one which selected mostly π^0 events.

The beam asymmetry shown in the left panels of Fig. 2 is the combination of both Compton and π^0 beam asymmetries (the minor contribution of events from other reactions can be
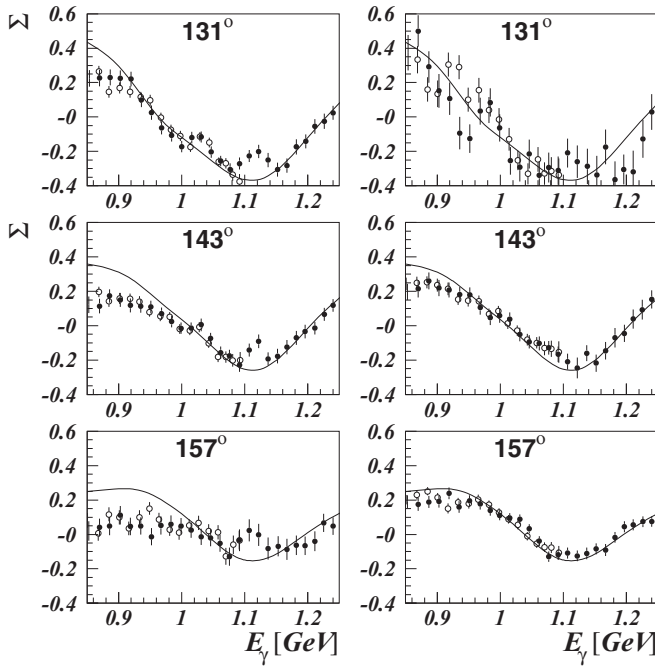
FIG. 2. Left: Beam asymmetry Σ for the mixture of Compton and π^0 events. Right: Beam asymmetry Σ obtained using side-band cuts (mostly π^0 events). Dark (open) circles are the results obtained with UV (green) laser. Solid lines are the SAID SM11 solution for the $\gamma p \to \pi^0 p$ beam asymmetry.

FIG. 3. Beam asymmetry Σ for Compton scattering on the proton. Dark (open) circles are the results obtained with UV (green) laser.

neglected)

$$\Sigma_{\text{tot}} = \alpha \Sigma_{\text{comp}} + (1 - \alpha)\Sigma_{\pi^0}, \tag{2}$$

where $\alpha = \frac{N_{\text{comp}}}{N_{\text{comp}} + N_{\pi^0}}$ denotes the fraction of Compton events.

The contamination of π^0 events was determined by normalizing the simulated π^0 spectrum in the angular bin of $157°$ to the experimental one in the region of the side-band cut (Fig. 1). Then the same normalization was used to determine the π^0 contamination in two other angular bins.

The fraction of Compton events α varied from $\sim90\%$ to $\sim40\%$ at 0.85 to 1.25 GeV in the angular bin $157°$, from $\sim75\%$ to $\sim35\%$ in the angular bin $143°$, and from from $\sim60\%$ to $\sim30\%$ in the angular bin $131°$. The π^0 beam asymmetry Σ_{π^0} was taken from the SAID SM11 solution. Then the Compton beam asymmetry Σ_{comp} was derived using Eq. (2) in which the π^0 beam asymmetry Σ_{π^0} was set equal to the SAID SM11 solution. The results are shown in Fig. 3. At the energies below 1 GeV the Compton beam asymmetry is close to 0. Above 1 GeV there are two narrow structures. They are better pronounced at $131°$ and almost degenerate at $157°$. This is a typical trend for the beam asymmetry Σ which *a priori* approaches 0 at $180°$.

Compton scattering was calculated by A. L'vov *et al.* [28] on the base of dispersion relations. The range of model validity is below 1 GeV. No calculation of Compton scattering at higher energies is available. Because of lack of theoretical predictions the data were fit in a simple way: The results from three angular bins were summed with weights proportional to inverse squares of their errors (lower right panel of Fig. 3) and fit
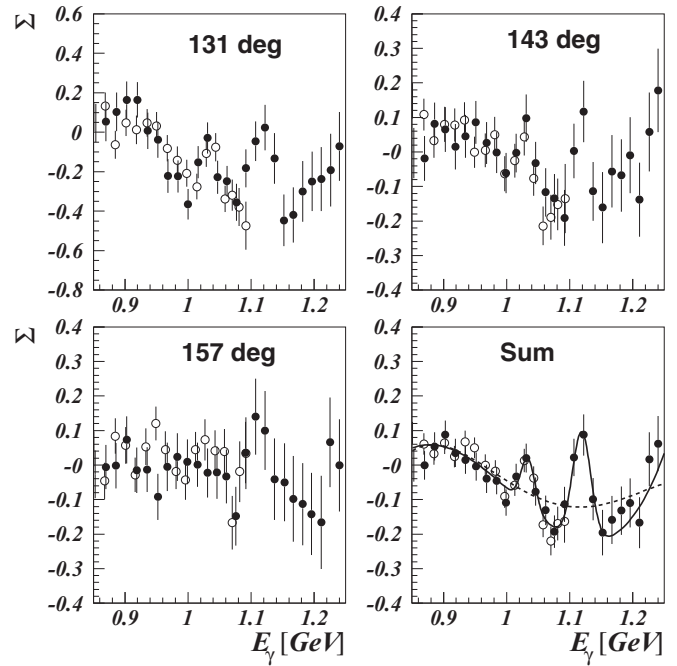
either by the 4-order polynomial (the background hypothesis) or by the 4-order polynomial-plus-two modified Breit-Wigner distributions (the background-plus-signal hypothesis). The formula for the Breit-Wigner distributions

$$A_i \frac{(E_\gamma - E_{Ri})\cos(\phi_i) + \Gamma_i \sin(\phi_i)}{(E_\gamma - E_{Ri})^2 + \frac{\Gamma_i^2}{4}}, \quad i = 1,2, \tag{3}$$

was suggested in Ref. [29] to describe the interference between a narrow resonance and background. The mass centers of the distributions were extracted as $E_{R_1} = 1.036 \pm 0.002$ GeV ($W_1 = 1.681$ GeV) and $E_{R_2} = 1.119 \pm 0.002$ GeV ($W_2 = 1.726$ GeV). The widths were $\Gamma_1 = 25 \pm 10$ and $\Gamma_2 = 35 \pm 12$ MeV ($\Gamma_1 = 18 \pm 6$ and $\Gamma_2 = 21 \pm 7$ MeV in the units of the center-of-mass energy W). The χ squares of the fits were 75.7/39 (background hypothesis) and 29.7/31 (signal-plus-background hypothesis). The log likelihood ratio of these two hypotheses ($\sqrt{2\ln(L_{B+S}/L_B)}$) corresponded to the confidence level of $\approx4.8\sigma$.

The errors shown in Fig. 3 are only statistical. The systematic uncertainty mainly originates from the determination of α. One may see from Eq. (2) that it less affects Σ_{comp} if (i) α is large and (ii) $\Sigma_{\text{comp}} \approx \Sigma\pi^0$. This uncertainty mostly affects Σ_{comp} in the regions of the observed structures. It results in the additional $\approx20\%$ errors in the extraction of the amplitudes A_i in Eq. (3).

The observation of the narrow structure at $W \approx 1.68$ GeV correlates with the previous results on η photoproduction [1–5], Compton scattering off the neutron [6], and η photoproduction on the proton [21,22]. The second structure at $W \approx 1.73$ GeV was not seen in the mentioned experiments. However, the modified SAID partial-wave analysis [10] hinted

two narrow P_{11} resonances at $W = 1.68$ GeV and $W = 1.73$ GeV. Both structures were also seen in the preliminary data on πN scattering by the EPECUR Collaboration [30]. The preliminary evidence for the peak at $W = 1.72$ GeV in $K\Lambda$ invariant mass was reported by the STAR Collaboration [31] but remains unpublished. The structure at $W \approx 1.68$ GeV is one more challenge for the explanation of the neutron anomaly in terms of the interference of well-known resonances [18]. This hypothesis cannot explain all experimental findings.

The energies $W \approx 1.68$ and $W \approx 1.73$ GeV correspond to the $K\Lambda$ and ωp photoproduction thresholds. This favors the cusp effect as an explanation of the neutron anomaly. Furthermore, a narrow step-like structure was also observed at the $K^*\Lambda$ threshold [32]. On the other hand it still remains unclear as to (i) why this effect is not seen in πN photoproduction, (ii) whether it could occur in Compton scattering, and (iii) why the structure at $W \approx 1.72$ GeV is seen in Compton scattering and is not seen in η photoproduction on the neutron.

The observation of these structures may signal one or two narrow resonances. Their masses and widths which stem from our simple fit are $M_1 = 1.681 \pm 0.002_{stat} \pm 0.005_{syst}$, $M_2 = 1.726 \pm 0.002_{stat} \pm 0.005_{syst}$ GeV, $\Gamma_1 = 18 \pm 6$, and $\Gamma_2 = 21 \pm 7$ MeV. The systematic errors ΔM are due to the accuracy of the calibration of the GRAAL tagging system.

The decisive identification of both structures requires a common fit of Compton and η photoproduction data. Accurate calculations of Compton scattering are needed for that. One particular task is to determine the waves and quantum numbers. Cusp is *a priori* an S-wave phenomenon. The chiral soliton model predicts one exotic P_{11} state with the mass near 1.7 GeV [13].

[1] V. Kuznetsov *et al.*, Phys. Lett. B **647**, 23 (2007).
[2] I. Jaegle *et al.*, Phys. Rev. Lett. **100**, 252002 (2008).
[3] I. Jaegle *et al.*, Eur. Phys. J. A **47**, 89 (2011).
[4] F. Miyahara *et al.*, Prog. Theor. Phys. Suppl. **168**, 90 (2007).
[5] D. Werthmüller *et al.*, Phys. Rev. Lett. **111**, 232001 (2013); Phys. Rev. C **90**, 015205 (2014).
[6] V. Kuznetsov *et al.*, Phys. Rev. C **83**, 022201 (2011).
[7] Ya. I. Azimov, V. Kuznetsov, M. V. Polyakov, and I. Strakovsky, Eur. Phys. J. A **25**, 325 (2005).
[8] A. Fix, L. Tiator, and M. V. Polyakov, Eur. Phys. J. A **32**, 311 (2007).
[9] K. S. Choi, S. I. Nam, A. Hosaka, and H. C. Kim, Phys. Lett. B **636**, 253 (2006).
[10] R. A. Arndt, Ya. I. Azimov, M. V. Polyakov, I. I. Strakovsky, and R. L. Workman, Phys. Rev. C **69**, 035208 (2004).
[11] T. Mart, Phys. Rev. D **83**, 094015 (2011).
[12] N. Isgur and G. Karl, Phys. Rev. D **18**, 4187 (1978); Phys. Lett. B **74**, 353 (1978); S. Capstick and W. Roberts, Prog. Part. Nucl. Phys. **45**, S241 (2000).
[13] D. Diakonov, V. Petrov, and M. V. Polyakov, Z. Phys. A **359**, 305 (1997).
[14] M. V. Polyakov and A. Rathke, Eur. Phys. J. A **18**, 691 (2003).
[15] D. Diakonov and V. Petrov, Phys. Rev. D **69**, 094011 (2004).
[16] J. R. Ellis, M. Karliner, and M. Praszalowicz, J. High Energy Phys. 05 (2004) 002; M. Praszalowicz, Acta Phys. Polon. B **35**, 1625 (2004); Ann. Phys. **13**, 709 (2004).
[17] D. Diakonov, V. Petrov, and A. A. Vladimirov, Phys. Rev. D **88**, 074030 (2013), and references therein.
[18] A. V. Anisovich *et al.*, Eur. Phys. J. A **41**, 13 (2009); V. Shklyar, H. Lenske, and U. Mosel, Phys. Lett. B **650**, 172 (2007); R. Shyam and O. Scholten, Phys. Rev. C **78**, 065201 (2008); V. Tryasuchev, Eur. Phys. J. A **50**, 120 (2014).
[19] M. Doring and K. Nakayama, Phys. Lett. B **683**, 145 (2010).
[20] E. F. McNicoll *et al.*, Phys. Rev. C **82**, 035208 (2010).
[21] V. Kuznetsov *et al.*, Acta Phys. Polon. B **39**, 1949 (2008).
[22] V. Kuznetsov and M. V. Polyakov, JETP Lett. **88**, 347 (2008).
[23] O. Bartalini *et al.*, Eur. Phys. J. A **33**, 169 (2007).
[24] It is worth to noting that the authors of Ref. [23] arrived at a different conclusion. Problems in their analysis are discussed in detail in Ref. [21].
[25] Detailed description of the GRAAL facility is available in O. Bartalini *et al.*, Eur. Phys. J. A **26**, 399 (2005).
[26] F. Ghio *et al.*, Nucl. Instrum. Methods Phys. Res., Sect. A **404**, 71 (1998).
[27] V. Kouznetsov *et al.*, Nucl. Instrum. Methods Phys. Res., Sect. A **487**, 396 (2002).
[28] A. I. L'vov, V. A. Petrun'kin, and M. Shumacher, Phys. Rev. C **55**, 359 (1997); A. L'vov (private communication).
[29] M. Amarian, D. Diakonov, and M. V. Polyakov, Phys. Rev. D **78**, 074003 (2008).
[30] A. Gridnev for the EPECUR Collaboration, PoS Hadron **2013**, 099 (2013).
[31] S. Kabana for the STAR Collaboration, presented at the 20th Winter Workshop on Nuclear Dynamics, Trelawny Beach, Jamaica, (2003) (unpublished).
[32] R. Ewald *et al.*, Phys. Lett. B **713**, 180 (2012).